SAND2022-15133C

Sandia National Laboratories

Exceptional service in the national interest

Calibrating Constitutive Models with Full-Field Data via Physics Informed Neural Networks

Craig M. Hamel, Sharlotte L.B. Kramer, and Kevin N. Long

2022 International Mechanical Engineering Conference and Exposition

Sandia National Laboratories is a multimission laboratory managed and operated by National Technology and Engineering Solutions of Sandia LLC, a wholly owned subsidiary of Honeywell International Inc. for the U.S. ...ation under contract DE-NA0003525.

Sandia National Laboratories is a multimission laboratory managed and operated by National Technology & Engineering Solutions of Sandia, LLC, a wholly owned subsidiary of Honeywell International Inc., for the U.S. Department of Energy's National Nuclear Security Administration under contract DE-NA0003525.

U.S. DEPARTMENT OF ENERGY

NNSA

Constitutive model calibration can require fewer tests when using full-field data, but current inverse methods for such calibration have several drawbacks

Experimental Data Requirements

Simple Tests

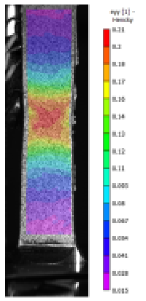

Tension

Notched Tension

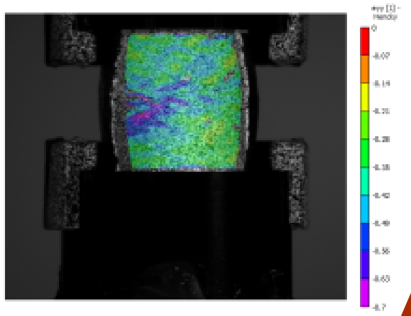

Compression

Complex Heterogeneous Tests

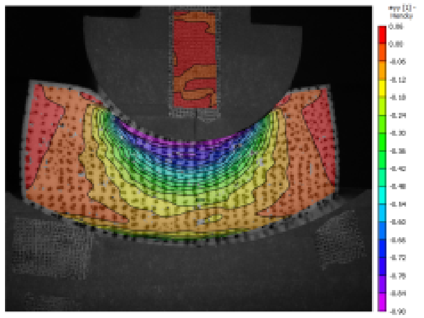

Impact with Round Indenter

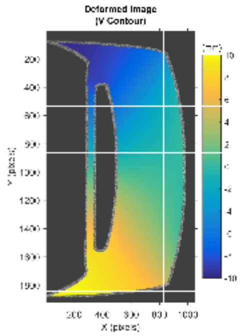

Tension of "D" Shaped Sheet

Example Inverse Methods

Finite Element Method Updating (FEMU):

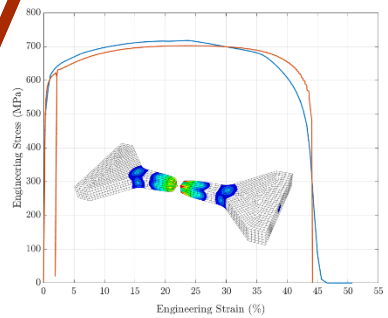

Kramer, et. al., IJF, 2019

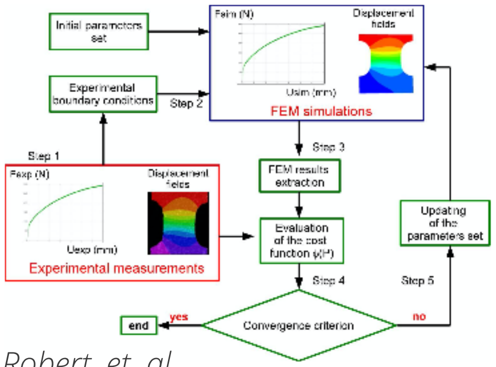

Robert, et. al.,
J. Strain Anal. Engr. Design, 2012

Virtual Fields Method (VFM):

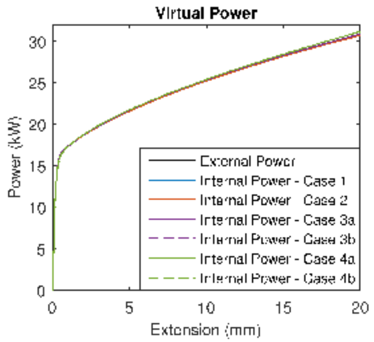

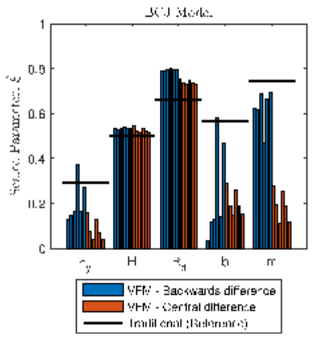

Jones, et. al., Sandia Report SAND2018-10635, 2018

Issues:

- Expensive and slow
- Hard to map surface data to FEM mesh
- Hard to use more than one experiment
- (VFM) Need volumetric strain data or plane-stress / sheet-material only limitation

Physics informed neural networks (PINNs) – elementary example

Burger's Equation

$$u_t + uu_x - (0.01/\pi)u_{xx} = 0, \quad x \in [-1, 1], \quad t \in [0, 1],$$

$$u(0, x) = -\sin(\pi x),$$

$$u(t, -1) = u(t, 1) = 0.$$

Residual

$$f := u_t + uu_x - (0.01/\pi)u_{xx}$$

NN loss function

$$MSE = MSE_u + MSE_f,$$

$$MSE_u = \frac{1}{N_u}\sum_{i=1}^{N_u} |u(t_u^i, x_u^i) - u^i|^2$$

$$MSE_f = \frac{1}{N_f}\sum_{i=1}^{N_f} |f(t_f^i, x_f^i)|^2$$

The "training data" here is the initial and boundary conditions at collocation points

Other points away from the boundaries are used to calculate the residual

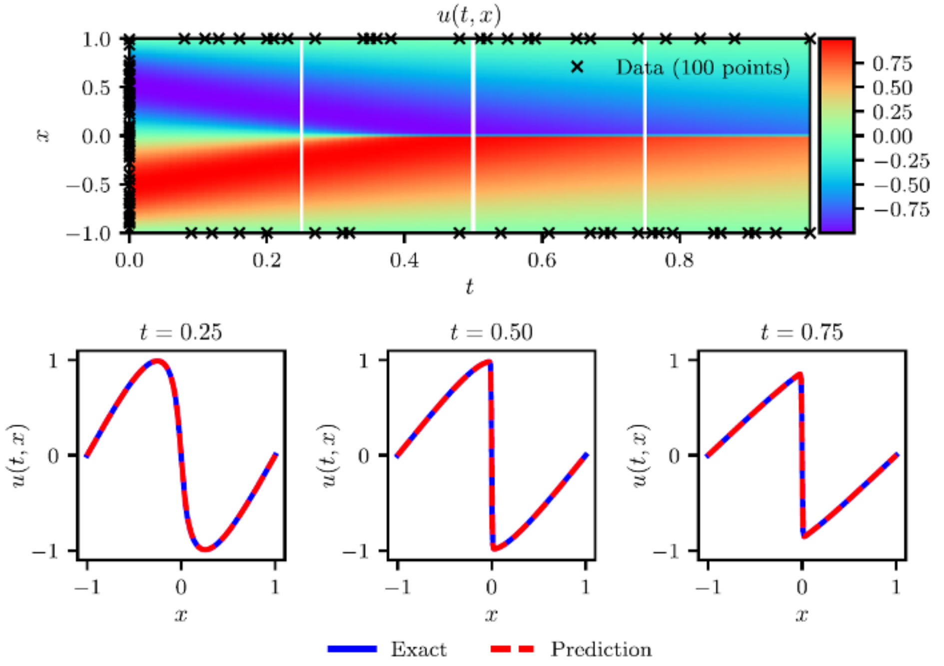

PINNs for solid mechanics – A few examples for the literature

Deep Energy Method for Finite-Strain Hyperelasticity

Nguyen-Thanh et. al., *Euro. J. Mechanics A*, 2020

Forward-Only Approach: U_x Field for Twisted Cuboid

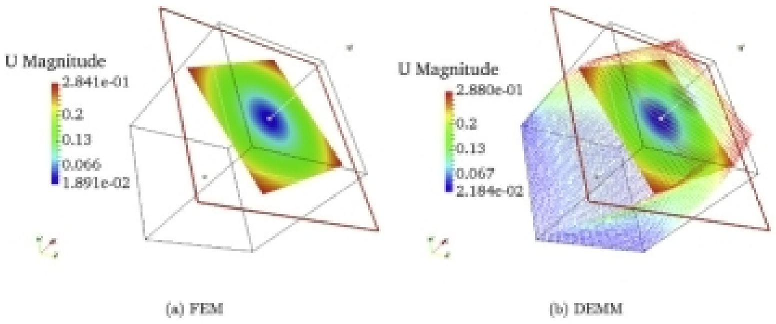

PINNs + Deep Energy Method to Resolve Stress Concentrations in Finite-Strain Hyperelasticity

Fuhg and Bouklas, *J. Comp. Phys.*, 2022

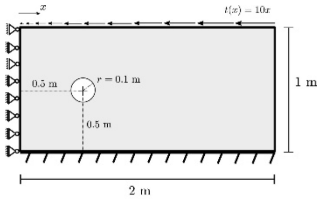

Beam with Deflection

Forward-Only Approach: U_x Field

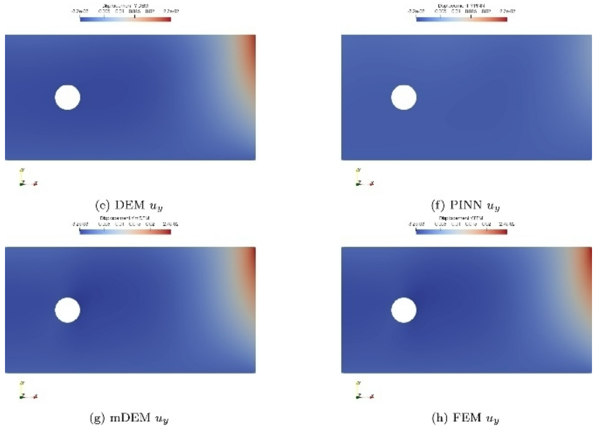

PINNs for Inverse Method for 2D Problems

Haghighat et. al., *CMAME* 2021

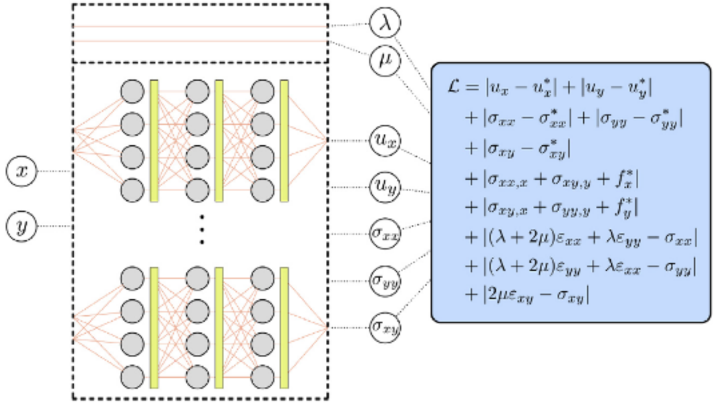

Separate PINN for each component of 2D stress and displacement

PINNs for Geometry Defect and Material Property Identification

Zhang et. al. *Science*, 2022

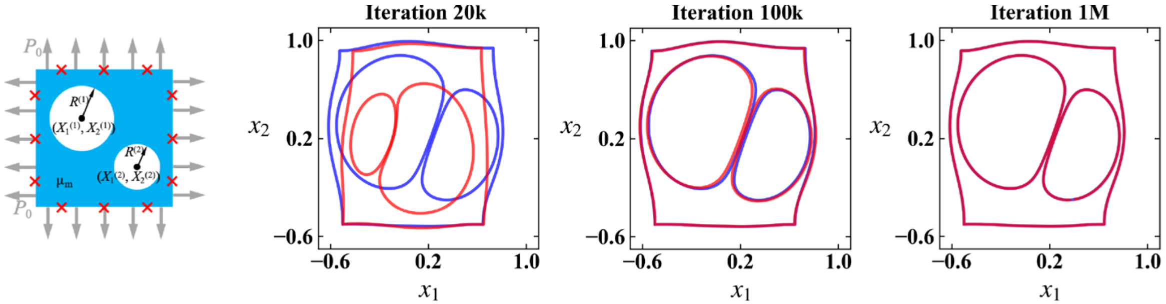

Shape estimation of PINN (red) vs. FEM (blue) for a hyperelastic material with increasing level of PINNs training

Our PINNs Approach – Theoretical Basis

Principle of Stationary Potential Energy

$$\Pi = \int_{\mathcal{B}_0} \psi(\mathbf{E})\, dv - \int_{\mathcal{B}_0} \mathbf{b} \cdot \mathbf{u} dv - \int_{\partial \mathcal{B}_0^{\mathbf{t}}} \tilde{\mathbf{t}} \cdot \mathbf{u} da, \qquad \min_{\mathbf{u} \in H^1(\mathcal{B}_0)} \Pi(\mathbf{u})$$

Basis for Deep Energy Method (DEM)

Principle of Virtual Work

$$\delta\Pi = \int_{\mathcal{B}_0} \delta\psi(\mathbf{E})\, dv - \int_{\mathcal{B}_0} \mathbf{b} \cdot \delta\mathbf{u} dv - \int_{\partial \mathcal{B}_0^{\mathbf{t}}} \tilde{\mathbf{t}} \cdot \delta\mathbf{u} da = 0$$

In the course of our work we found issues with both of these descriptions in the realm of PINNs

The principle of stationary potential energy was robust, but would leave internal forces out of balance

The principle of virtual work had slower convergence but balanced forces to reasonable tolerances

We therefore sought a balance between these (A weak form version of gradient enhanced PINNs)

Our PINNs approach to material model calibration utilizes heterogenous full-field data and global force data.

Kinematics

Displacement BC

Neural network

$$\mathbf{u}_{\mathcal{N}}\left(\mathbf{X},t\right) \approx \tilde{\mathbf{u}}\left(\mathbf{X},t\right) + f\left(\mathbf{X}\right)\mathcal{N}\left(\mathbf{X},t\right)$$

$$\mathbf{F}^e_{\mathcal{N}} = \mathbf{I} + \nabla_{\mathbf{X}}\mathbf{u}^e_{\mathcal{N}}$$

$$\nabla_{\mathbf{X}}\mathbf{u}^e_{\mathcal{N}} = \sum_{I=1}^{N_{nodes}} \mathbf{u}^I_{\mathcal{N}} \otimes \nabla_{\mathbf{X}} N^I$$

Standard shape functions for Hex8 elements

Total potential energy for time step n

$$\Pi^n_{\mathcal{N}} = \sum_{e=1}^{N_e}\sum_{q=1}^{N_q} w_q \left(\det \mathbf{J}^e\right)\psi^e\left(\mathbf{F}^e_{\mathcal{N}}\right)$$

Internal Force Vector

$$\mathbf{f}_{\mathcal{N}} = \delta\Pi_{\mathcal{N}} = \frac{\partial \Pi_{\mathcal{N}}}{\partial \mathbf{u}_{\mathcal{N}}}$$

Total loss function $\mathcal{L} = \beta\mathcal{L}_r + \gamma\mathcal{L}_{\mathbf{u}} + \delta\mathcal{L}_f$

Loss function for potential energy $\mathcal{L}_r = \Pi_{\mathcal{N}} + \alpha\|\delta\Pi_{\mathcal{N}}\|^2_{free}$

For inverse problems we have the additional error terms for experimental data

Surface Displacement Error

$$\mathcal{L}_{\mathbf{u}} = \frac{1}{N_{\mathbf{u}}}\sum_{i=1}^{N_{\mathbf{u}}} \|\mathbf{u}_{\mathcal{N}}\left(\mathbf{X}^*_i, t^*_i\right) - \mathbf{u}^*_i\left(\mathbf{X}^*_i, t^*_i\right)\|^2$$

Global Force Error

$$\mathcal{L}_f = \frac{1}{N_t}\sum_{n=1}^{N_t} \|f_{net}\left(t_n\right) - f^*_{net}\left(t_n\right)\|^2$$

Schematic of PINN architecture

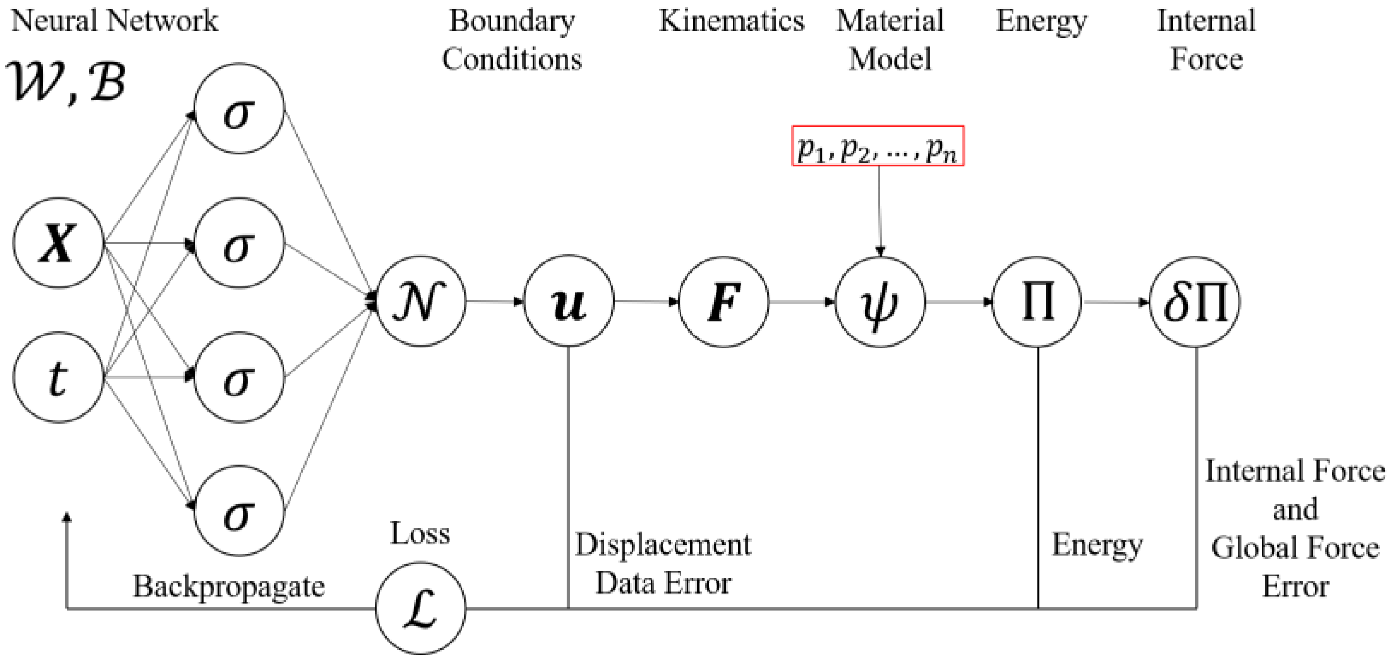

Training Details

- 3 hidden layer feed forward neural network with 50 neurons per hidden layer
- Hyperbolic tangent activation functions
- Adam optimizer with a learning rate of 0.001
- Exponential decay learning rate scheduler
- Xavier initialization used for NN weights and biases
- Material parameters are initialized randomly between a lower and upper bound

As a validation exercise, our PINNs architecture used in the forward problem reasonably approximates displacements and global forces for several hyperelastic models in large deformation BVPs.

Forward problem code-to-code V&V using Neo-Hookean constitutive model

Global force

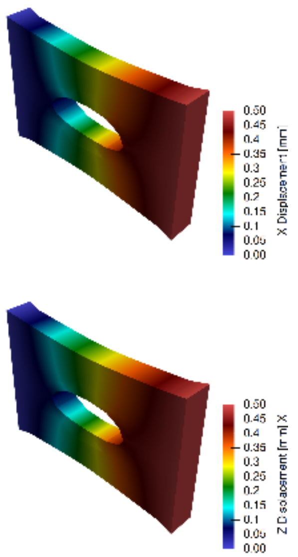

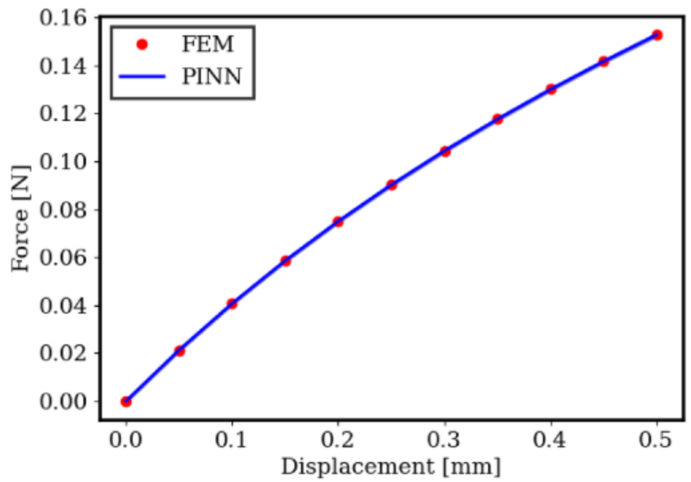

$$\psi(\mathbf{C}) = \frac{1}{2}K\left[\frac{1}{2}\left(J^2-1\right)-\ln J\right]+\frac{1}{2}\mu\left(\bar{I}_1-3\right)$$

Forward problem code-to-code V&V using Gent constitutive model

Global force

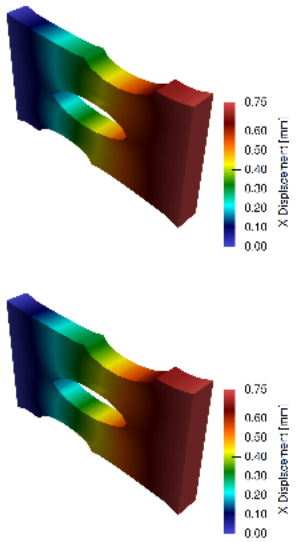

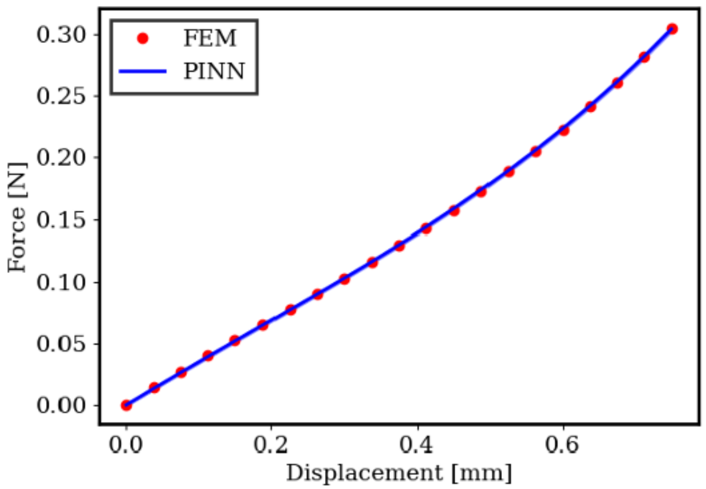

$$\psi(\mathbf{C}) = \frac{1}{2}K\left[\frac{1}{2}\left(J^2-1\right)-\ln J\right]-\frac{1}{2}\mu J_m \ln\left(1-\frac{\bar{I}_1-3}{J_m}\right)$$

Forward problem example - Neohookean

Displacement components at 50% global strain

FEM

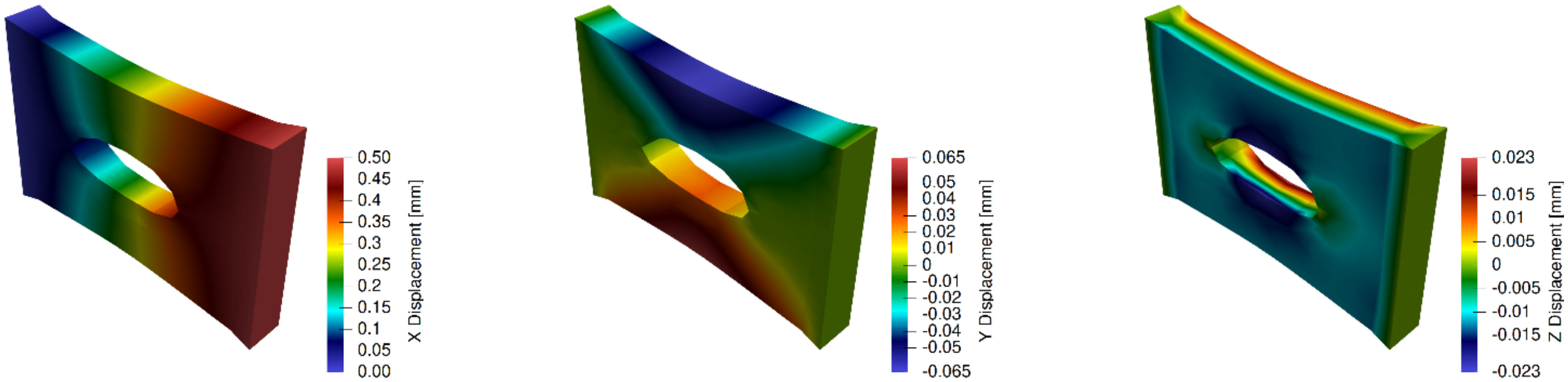

PINN

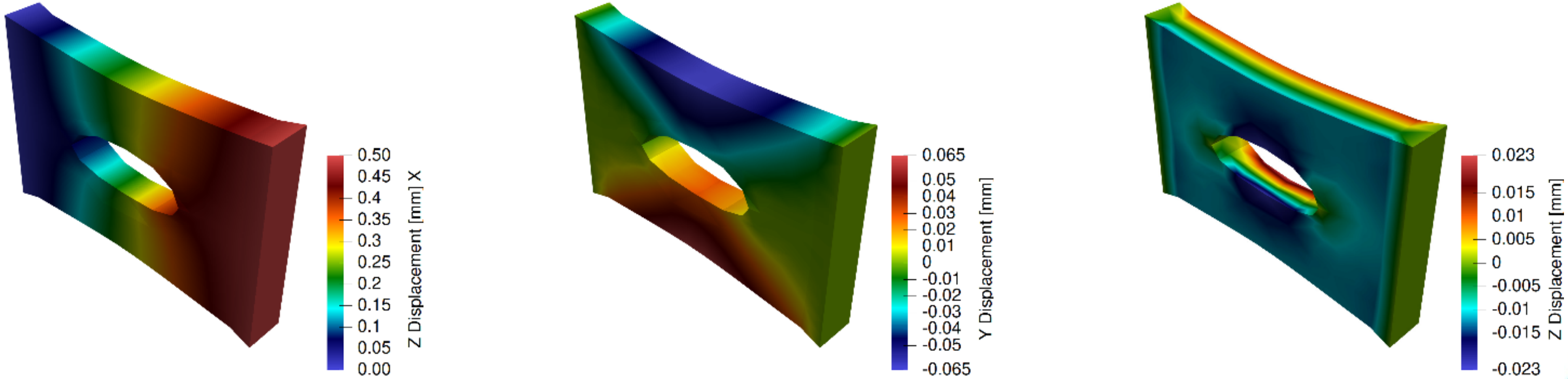

Forward problem example - Gent

Displacement components at 75% global strain

FEM

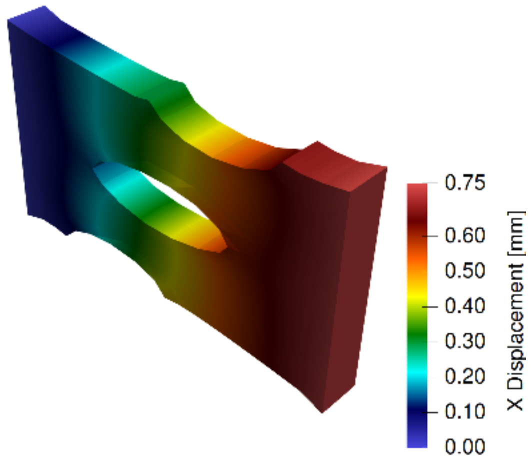

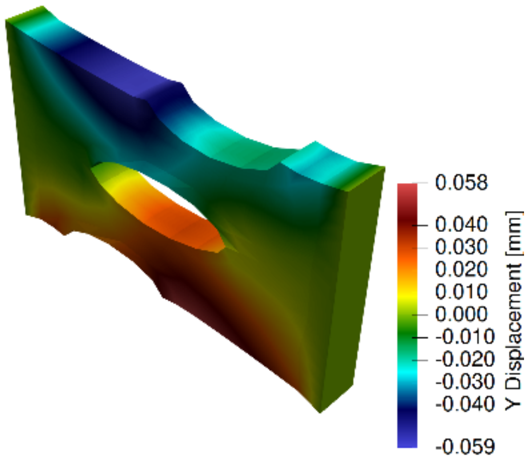

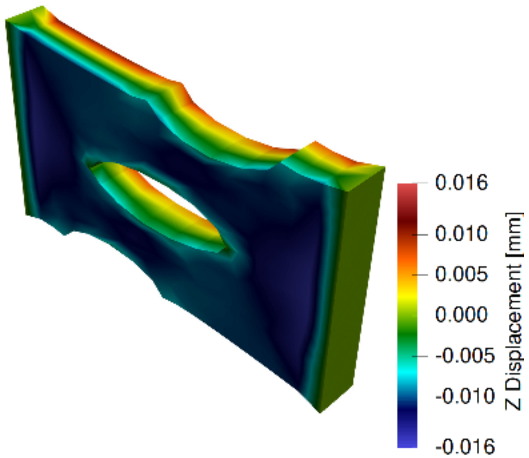

PINN

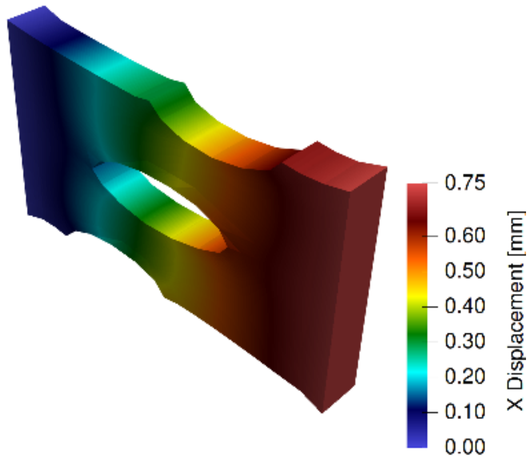

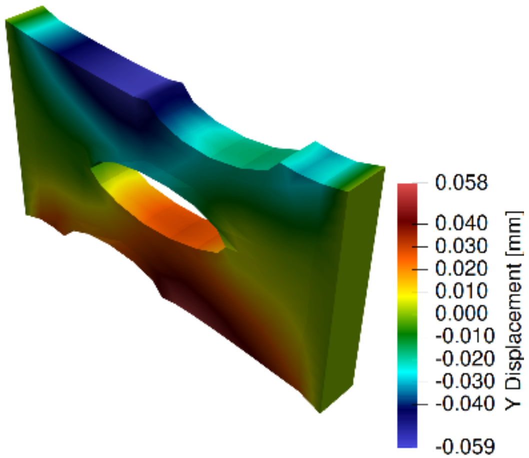

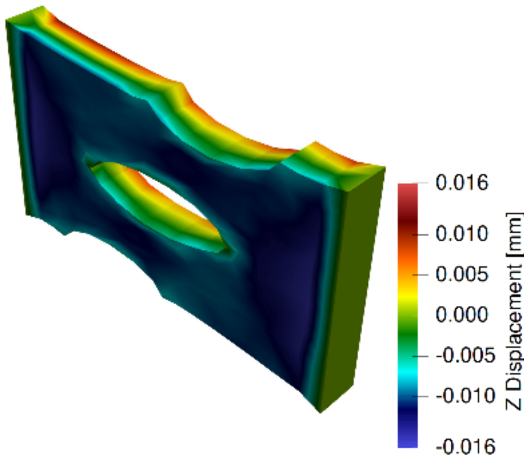

Synthetic data inverse problem workflow

Mesh geometry of experimental specimen and run FEA

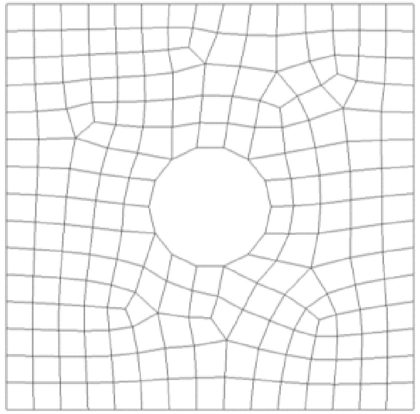

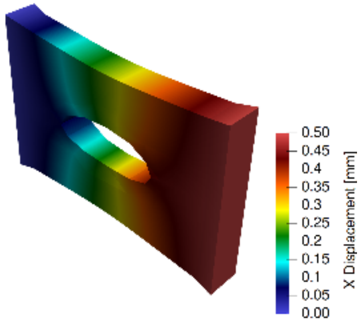

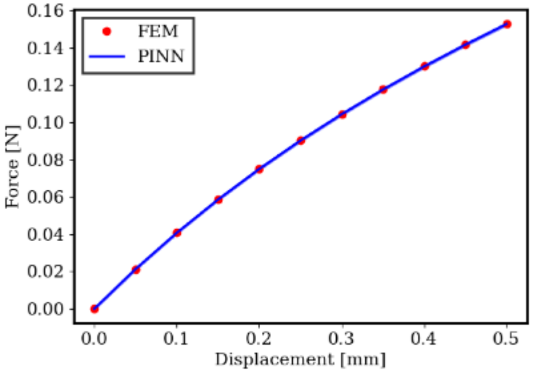

Feed data into PINN training loop

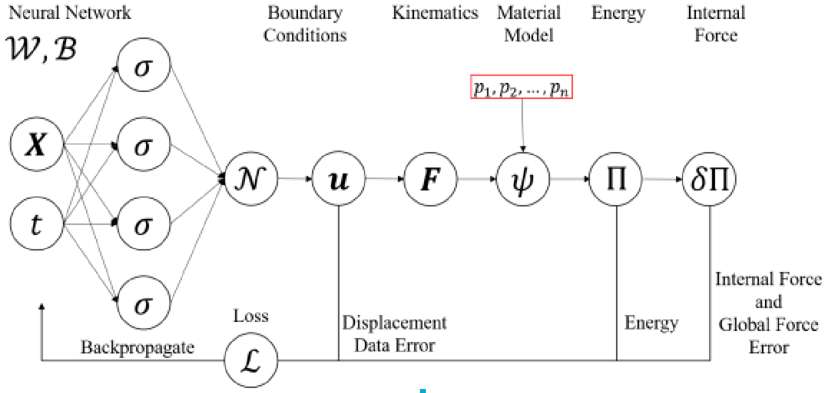

Output optimized constitutive model parameters

$$\psi(\mathbf{C}) = \frac{1}{2} K \left[\frac{1}{2} \left(J^2 - 1 \right) - \ln J \right] + \frac{1}{2} \mu \left(\bar{I}_1 - 3 \right)$$

Here, the surface displacement data aligns exactly with the computational mesh used to calculate integrals in the PINN loss function

Inverse problem example - Neohookean

8 separate PINNs are trained to show repeatability

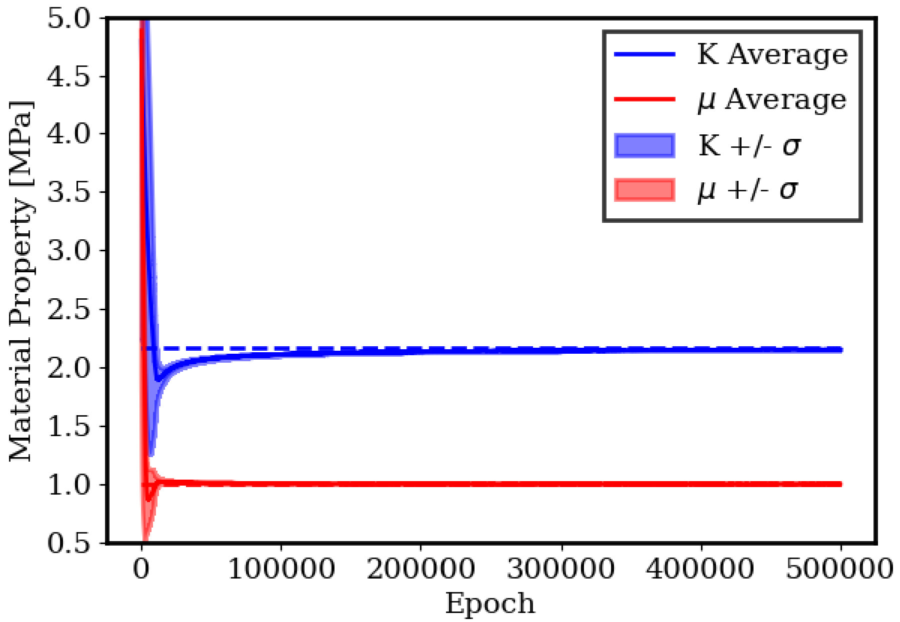

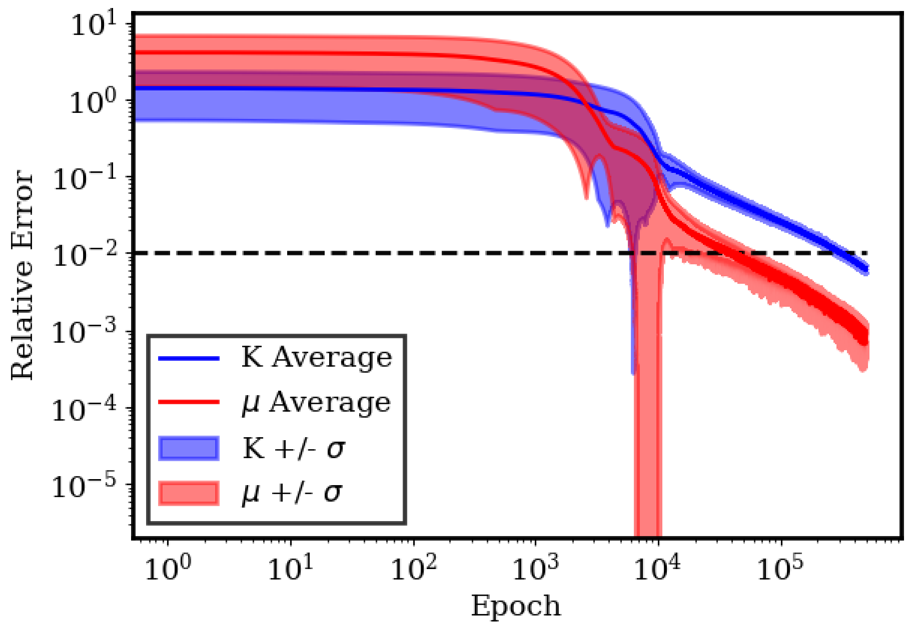

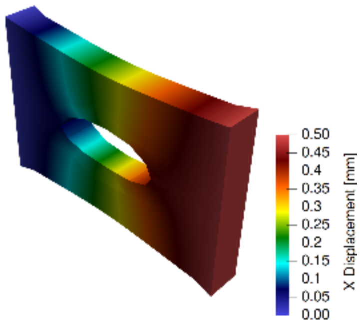

$$\psi\left(\mathbf{C}\right) = \frac{1}{2}K\left[\frac{1}{2}\left(J^2 - 1\right) - \ln J\right] + \frac{1}{2}\mu\left(\bar{I}_1 - 3\right)$$

Here the computational mesh nodes and surface displacement data point locations line up

Inverse problem example - Gent

8 separate PINNs are trained to show repeatability

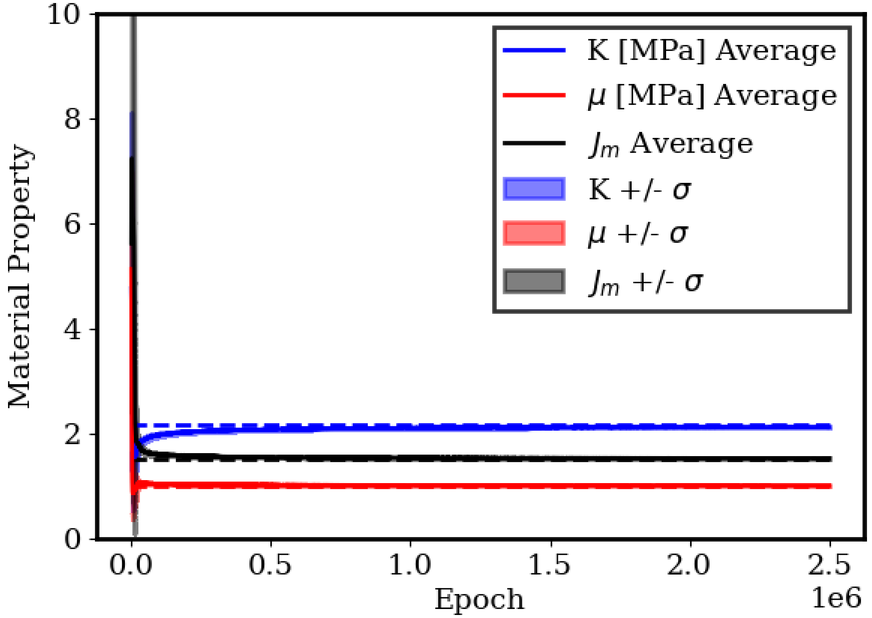

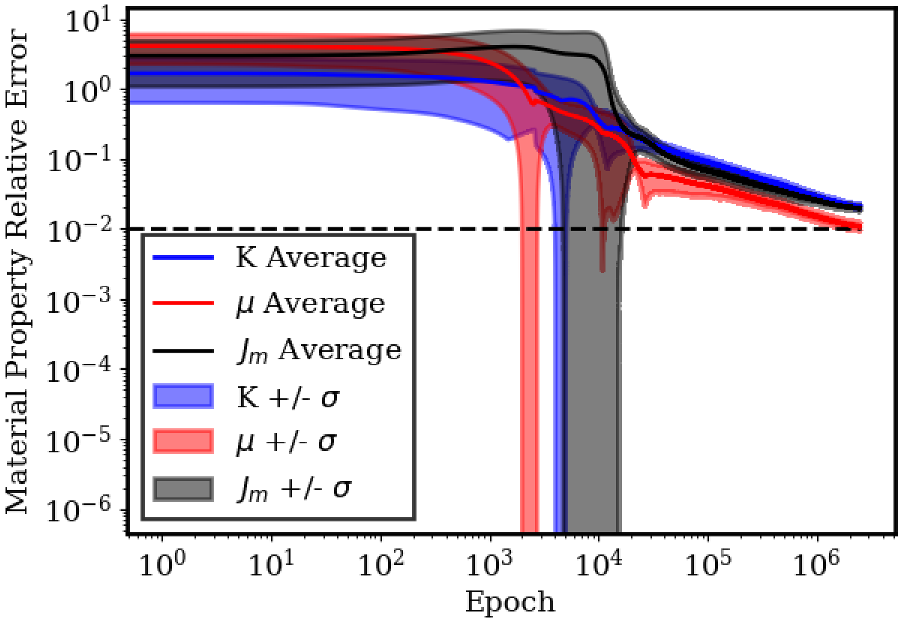

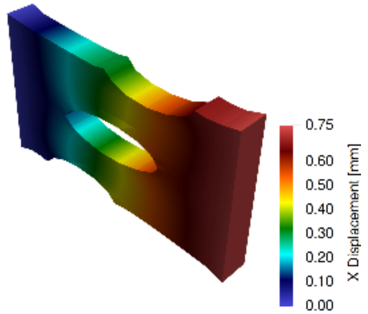

$$\psi\left(\mathbf{C}\right) = \frac{1}{2}K\left[\frac{1}{2}\left(J^2-1\right)-\ln J\right]-\frac{1}{2}\mu J_m \ln\left(1-\frac{\bar{I}_1-3}{J_m}\right)$$

Here the computational mesh nodes and surface displacement data point locations line up

Inverse problem example – Neohookean with data dropout

Mesh geometry of experimental specimen and run FEA

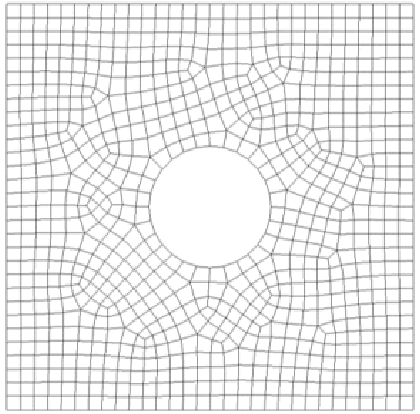

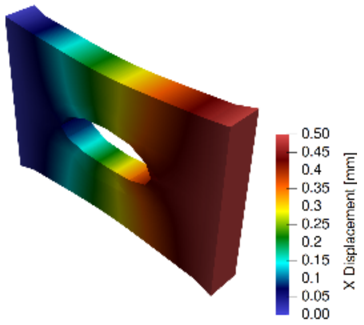

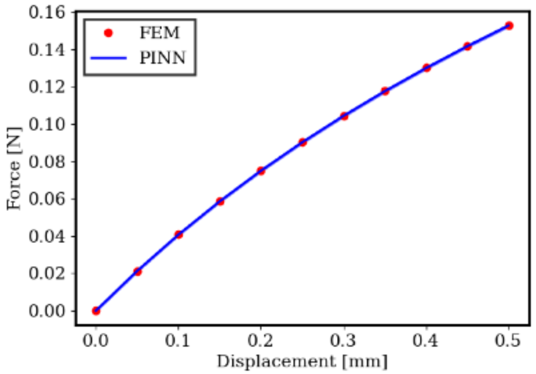

Feed data into PINN training loop

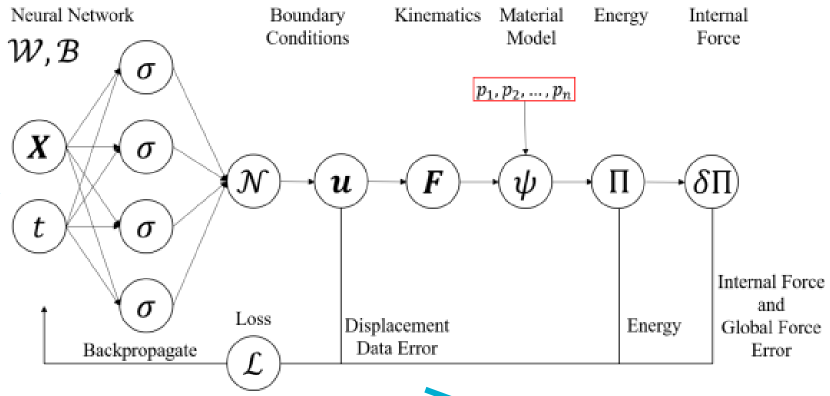

Use a coarse mesh for calculating integrals

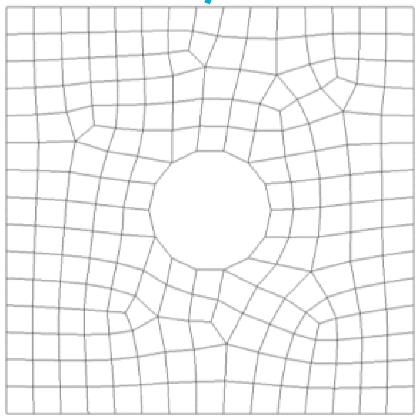

Output optimized constitutive model parameters

$$\psi(\mathbf{C}) = \frac{1}{2} K \left[\frac{1}{2} \left(J^2 - 1 \right) - \ln J \right] + \frac{1}{2} \mu \left(\bar{I}_1 - 3 \right)$$

Here, the surface displacement data do not align with the computational mesh used to calculate integrals in the PINN loss function

Inverse problem example – Neohookean with data dropout

Bulk Modulus

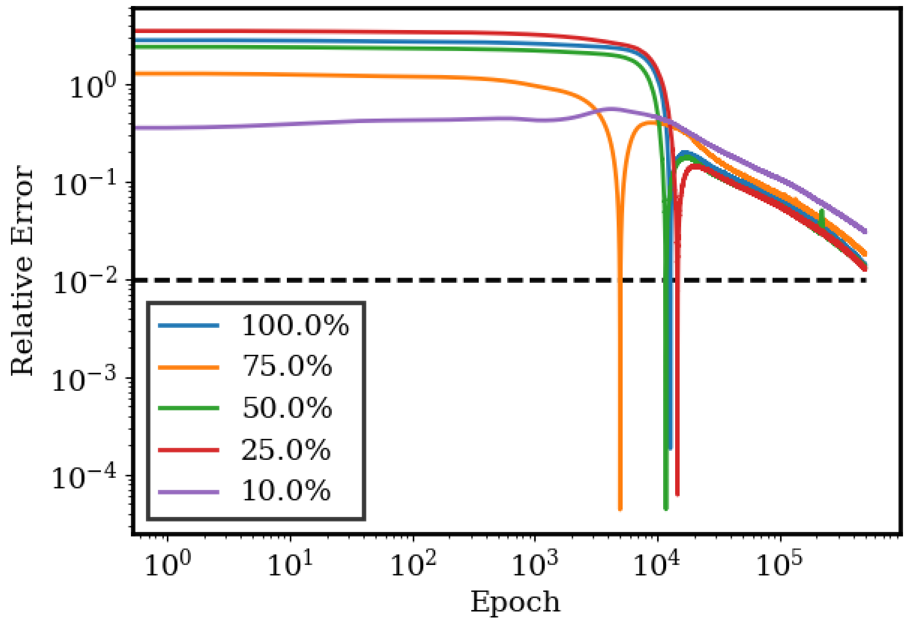

Shear Modulus

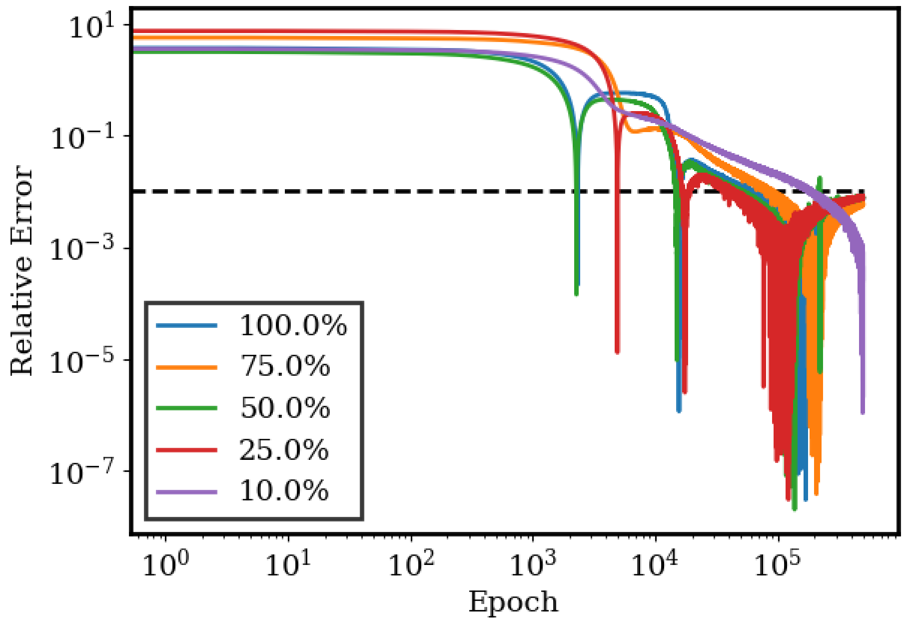

$$\psi\left(\mathbf{C}\right) = \frac{1}{2}K\left[\frac{1}{2}\left(J^2 - 1\right) - \ln J\right] + \frac{1}{2}\mu\left(\bar{I}_1 - 3\right)$$

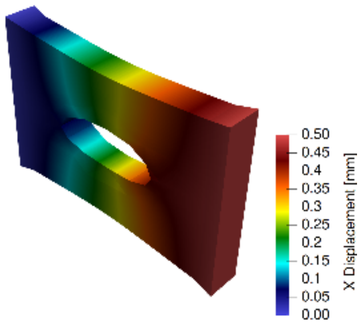

Data points are randomly dropped to mimic uncorrelated DIC data

Here the computational mesh nodes and surface displacement data point locations do not line up

Inverse problem example – Neohooken with contiguous data dropout

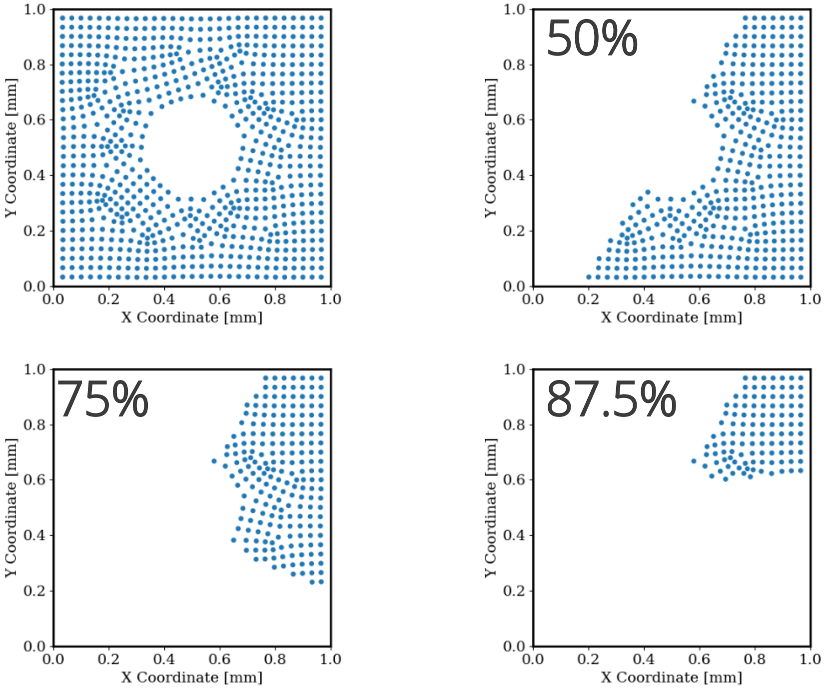

Remove large contiguous regions of synthetic DIC data to mimic a poor speckle pattern, region out of focus, or other experimental defects/artifacts

Bulk Modulus

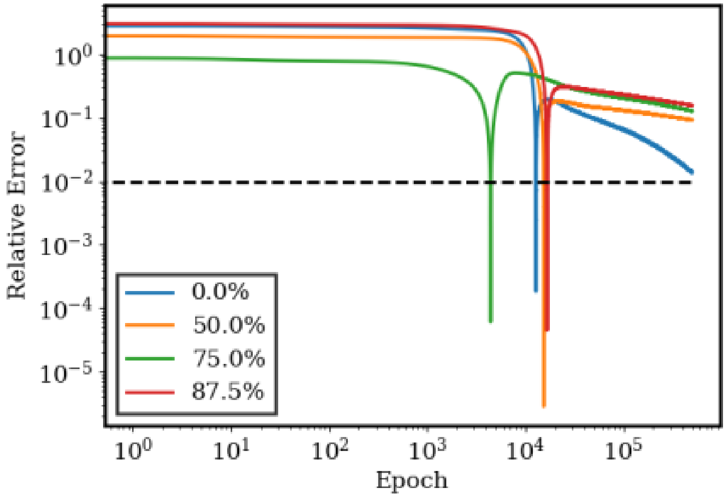

Shear Modulus

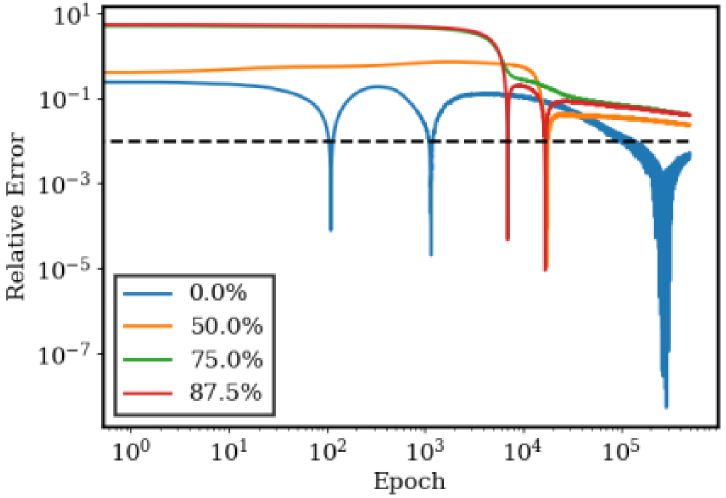

$$\psi(\mathbf{C}) = \frac{1}{2}K\left[\frac{1}{2}\left(J^2 - 1\right) - \ln J\right] + \frac{1}{2}\mu\left(\bar{I}_1 - 3\right)$$

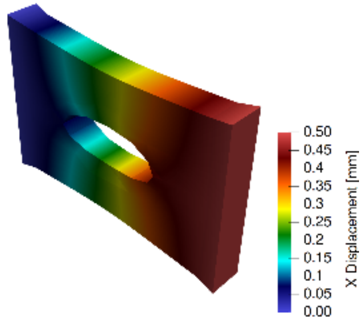

Conclusion

1. An approach for calibrating constitutive models with full-field data using PINNs was developed
2. This approach was shown to be able to successfully calibrate Hyperelastic constitutive models
3. With this approach, we relaxed the difficulty of interpolating DIC data onto a FEM mesh
4. Although initially successful, the following needs to be addressed
   a) Improved training
   b) Incorporation of multiple experimental test specimens into the training process
   c) Extension to material models with history dependence
   d) Incorporation of inertial affects for leveraging dynamic experimental tests
   e) Contact